JOURNAL OF MATERIALS SCIENCE 27 (1992) 448–452

Characterization of crystal phases, morphology and crystallization processes in lithium aluminosilicate glass–ceramic

C. CANTALINI, M. PELINO*
Department of Chemistry, Chemical Engineering and Materials, University of L'Aquila, 67040 Monteluco di Roio, L'Aquila, Italy

The nucleation and crystallization processes of Li_2O–Al_2O_3–SiO_2 glass–ceramics were investigated by differential thermal analysis. The crystalline phases produced during thermal treatment at different temperatures and the residual glassy phase were characterized by X-ray diffraction, SEM and image analysis techniques. The activation energy of the crystallization process was calculated as $E = 380 \pm 20$ kJ mol^{-1}. The influence of nucleating agents (TiO_2, ZrO_2) was evaluated to obtain glass–ceramics transparent to visible light. The stability of the glassy phase in cooling was determined by means of temperature–time–transformation curves.

1. Introduction

The glass–ceramics (GCs) obtained by controlled crystallization of lithium aluminosilicate glasses (G) exhibit a very low, zero, or even negative thermal expansion coefficient (TEC) in a wide temperature range [1, 2]. This characteristic is due to the highly anisotropic TEC of β-eucryptite (structurally similar to β-quartz) and β-spodumene solid solutions. The former shows an increase of TEC along the *a* axis and a decrease along the *c* axis with increasing temperature; the latter shows the opposite behaviour [3]. The net result is a low or negative expansion. The final TEC of the GC material is a combination of the thermal expansions of the crystalline and the residual glassy phases. Therefore, in defining the TEC of the GC, the chemical composition and the thermal treatment of the parent G, the nature of the precipitated phases and the ratio G/GC are the guide factors.

Another relevant feature of this kind of GC is the possibility of obtaining transparency to visible light. To accomplish this feature, the kinetics of crystallization of the parent G plays an important role because a strong nucleation tendency, i.e. an elevated number of nucleating embroys per unit volume, is necessary for obtaining fine crystal grains, inferior in dimensions to visible light wavelengths [4]. This tendency, on the other hand, decreases the resistance of the parent G to devitrification, so that undesirable crystallization may occur during the G formation process.

In obtaining a transparent GC it is necessary to investigate the nucleation mechanism, which is mainly influenced by the kind and percentage of nucleating agents as well as by the morphology and dimensions of the precipitated crystalline phases.

The chemical composition of the parent G plays an important role; the correct percentages of network-forming Si and Al, interstitial substituents (Li, Zn, Mg, etc.) and network modifiers (Ca, Na, K, etc.), must be adjusted according to the most appropriate phase and glass-formation diagrams and, eventually, to the technological aspects of production. It turns out that different variables, but reciprocally influenced, must be taken into consideration in tailoring the properties of a low-TEC transparent lithium aluminosilicate GC.

This paper reports the preliminary results obtained by X-ray diffraction (XRD), differential thermal analysis (DTA), SEM and image analysis techniques on the crystallization process of lithium aluminosilicate GC nucleated with TiO_2 and ZrO_2. The stability of the G phase was also investigated and depicted as a function of temperature and time (T–T–T curves).

2. Experimental procedure

The G samples were prepared by melting in a platinum crucible approximately 100 g of reagent-grade chemicals: quartz sand, $Al(OH)_3$, LiOH, $MgCO_3$, CaO, K_2CO_3, $BaCO_3$, TiO_2, ZrO_2 and As_2O_3.

The powders were homogenized in a rotating mixer for 20 min and melted for 11 h in a Superkantal programmable electric furnace at a temperature of 1600 °C. The batch was quenched in doubly-distilled water and the G was crushed and remelted for 2 h. The molten batch was then quenched in water or poured on to a graphite plate to obtain 3 mm thick, 45 mm diameter discs.

---

* To whom correspondence must be addressed.

0022–2461/92 $03.00 + .12

DTA was performed on the powdered G at heating rates of 5, 10, 20 and 40 °C min^{-1}. All the G samples prepared and the respective crystallized samples were subjected to XRD analysis in order to investigate the amorphous phase and to determine the nature and amount of the crystalline phase.

The GCs were prepared for microscopic observation, to highlight the grain size and morphology of the crystalline phase, by etching the polished surface with 2% HF, for times ranging from 10 to 60 s. Optical, SEM and image analysis (Quantimet 970) were carried out in order to determine the morphology of the crystalline phase.

The Quantimet 970 was also employed for evaluating the percentage of the crystalline phase with respect to the glassy one. This was performed by comparing (on several pictures for each sample) the volume of the crystals with that of the voids (G phase) left by the HF chemical etching. The results were stored and processed by the instrument's software.

3. Results and discussion

The percentages of the various oxides employed in defining the composition of the GC are listed in Table I. The differences between the four compositions (A, B, C, D) reside in the percentages of TiO_2 and ZrO_2, added as nucleating agents for the heterogeneous crystallization [5], and in the corresponding variation of the SiO_2 content. The Ba, K and Ca oxides, because of their action as network-modifiers, were added in order to lower the melting temperature of the G and its viscosity. The As_2O_3 was required as a refining agent of the batch. The criteria for selection of the various oxides, composition ranges were based on the glass-formation diagram [1] and on the data available in the literature for systems suitable to form low-TEC and transparent lithium aluminosilicate GC.

3.1. Differential thermal analysis

Fig. 1 shows a comparison of the DTA curves obtained for glasses A, B, C, D at 10 °C min^{-1} heating rate by means of a computerized Netzsch STA model 409. The temperatures indicated in the figure are relative to the top of the peak and show a decreasing trend with increasing amount of nucleating agents. The only anomaly is trace A, which shows a broad peak with an approximate maximum at 860 °C. This behaviour was attributed to the prevalence of surface crystallization over the bulk phenomenon, which is unfavourable because of the inadequate amount of nucleating agents. Fig. 2 shows the DTA traces for the D composition obtained at different heating rates. From these graphs the activation energy of the crystallization process can be calculated through the

TABLE I List of the various oxides employed in defining the four compositions investigated

Oxide	Oxide content (wt %)			
	A	B	C	D
SiO_2	62.25	62.00	61.00	60.50
Al_2O_3	21.20	21.20	21.20	21.20
Li_2O	2.80	2.80	2.80	2.80
MgO	1.00	1.00	1.00	1.00
ZnO	6.10	6.10	6.10	6.10
K_2O	0.40	0.40	0.40	0.40
CaO	0.60	0.60	0.60	0.60
BaO	1.60	1.60	1.60	1.60
TiO_2	1.75	1.75	2.50	2.50
ZrO_2	1.50	1.75	2.00	2.50
As_2O_3	0.80	0.80	0.80	0.80

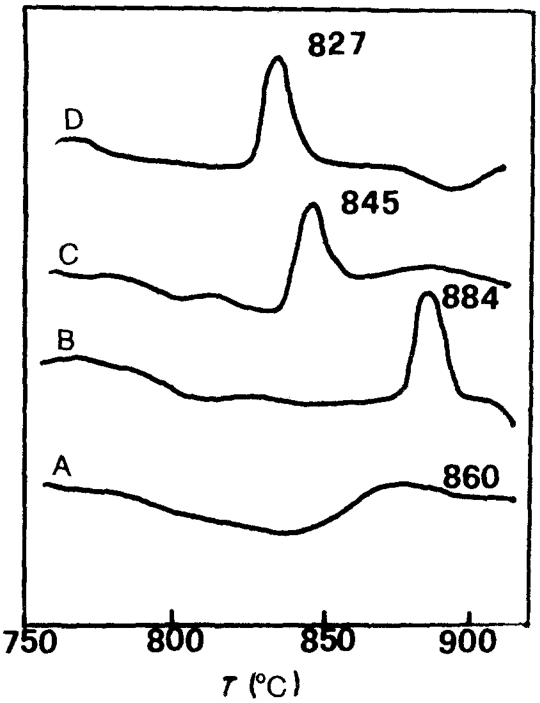

Figure 1 DTA at 10 °C min^{-1} of the glass compositions (A, B, C, D) investigated.

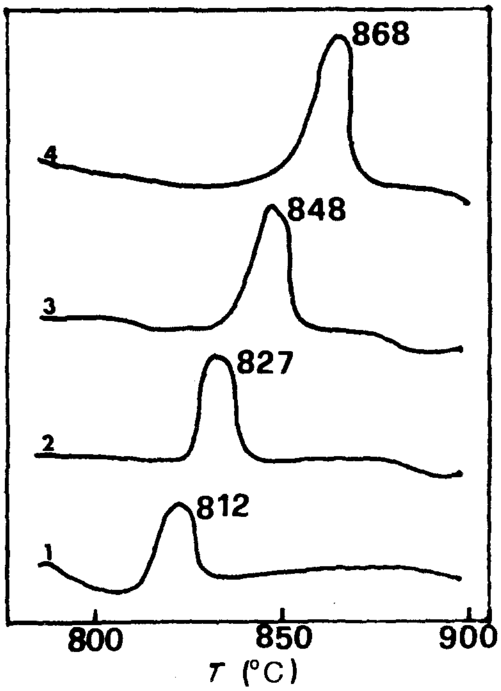

Figure 2 DTA at (1) 5 °C min^{-1}, (2) 10 °C min^{-1}, (3) 20 °C min^{-1}, (4) 40 °C min^{-1}, of D composition glass–ceramic.

equation

$$\log \beta = \frac{E}{19.1(1/T_p)} + A$$

where β is the heating rate (°C min^{-1}), E is the activation energy, T_p is the temperature of crystallization (K) and A is a constant [6, 7].

In Table II are reported the experimental data from which, by least-squares analysis, the activation energy was computed, $E = 380 \pm 20$ kJ mol^{-1}. The associated uncertainty is an overall estimation of the errors relative to the determination of T_p and the standard deviation from the mean.

On the basis of the DTA traces, the crystallization temperature has been inferred as 830 ± 10 °C, assuming the beginning of the crystallization process to be somewhat lower than the top of the exothermic peak.

The other exothermic peak, due to the precipitation of $ZrTiO_4$ [8], was not sharply detected, probably because the amount of heat evolved in the process was below the sensitivity of the instrumentation. A calorimetric measurement [3] would probably have been able to detect the heat evolved. The nucleation temperature was set at 740 ± 10 °C, since this value emerged as the most appropriate in promoting an efficient crystallization.

3.2. X-Ray diffraction

Samples of G of the four compositions were analysed by XRD in order to detect crystallization during the quenching or the casting on to graphite of the molten G. All the samples were found to be amorphous. The same samples of G were analysed, after the nucleation and crystallization thermal treatments (in the above-mentioned range), for the characterization of the crystalline phases. Fig. 3 shows a spectrogram of the GC composition D. The diffraction peaks were identified as $LiAlSi_2O_6$, with β-quartz crystal structure. A similar pattern was also obtained for A, B and C compositions of GC.

The stability of the G phase was verified by the T–T–T diagram for the B composition. The degree of crystallinity was evaluated by XRD. The T–T–T curve is depicted in Fig. 4 where, for the sake of clearer representation, only the first point of crystallinity is reported (triangles in the figure) even if the samples were held at each experimental temperature for a time of up to 10 h.

3.3. SEM and image analysis

The four compositions of GC, obtained by means of the same thermal treatment, were observed by optical microscopy. The GCs of composition C and D were completely transparent, while the two others, A and B, showed different and non-reproducible degrees of opacity. The SEM observation and the image analysis of the micrographs highlighted the fact that the average crystal grain size of compositions A and B (Fig. 5) was of the order of 1 μm, while for C and D compositions (Fig. 6) it was of the order of 0.1 μm. Therefore only the latter grain size was smaller than visible light wavelengths.

TABLE II Parameters employed in the calculation of the activation energy

β (°C min^{-1})	$\log\beta$	T_p (K)	$10^4/T_p$ (K^{-1})
5	0.699	1085.1	9.216
10	1.000	1099.6	9.094
20	1.301	1120.4	8.925
40	1.602	1140.7	8.767

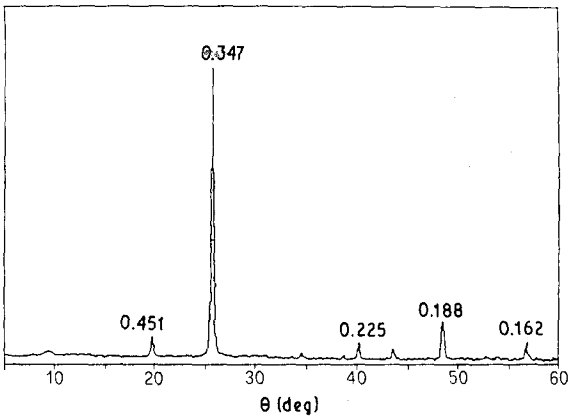

Figure 3 X-ray spectrogram of D composition glass–ceramic; peak spacings in nm.

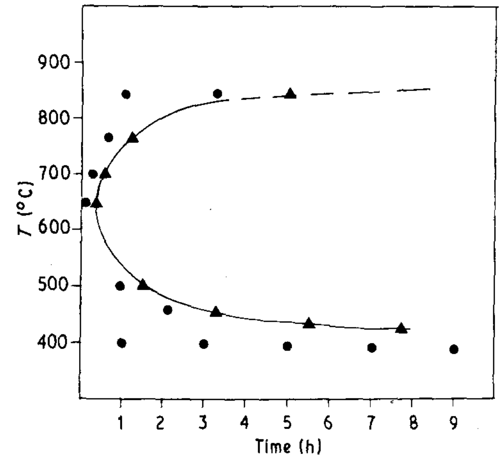

Figure 4 Temperature–time–transformation (T–T–T) curve for B composition glass: (▲) crystalline, (●) amorphous.

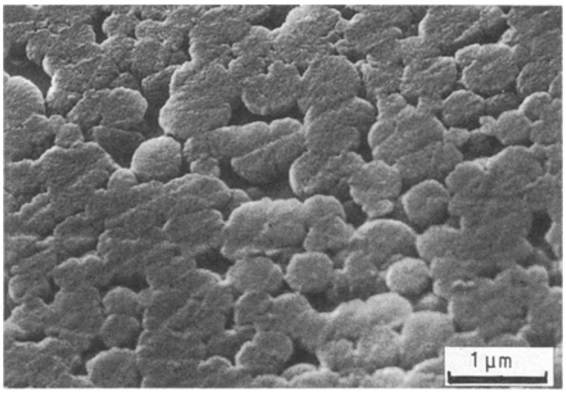

Figure 5 SEM micrograph of B composition glass–ceramic etched in 2% HF for 10 s.

TABLE III Nucleation temperature (T_n) and time (τ_n), crystallization temperature (T_c) and time (τ_c), and relative percentage of crystalline phase (%CPh)

T_n (°C)	τ_n (min)	T_c (°C)	τ_c (min)	$\ln \tau_c$	%CPh
740	60	830	10	2.30	76
740	60	830	20	2.99	84
740	60	830	30	3.40	89
740	60	830	40	3.68	93
740	60	830	50	3.91	95

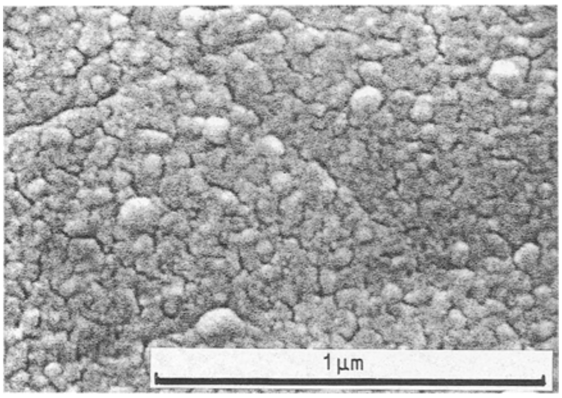

Figure 6 SEM micrograph of D composition glass–ceramic etched in 2% HF for 10 s.

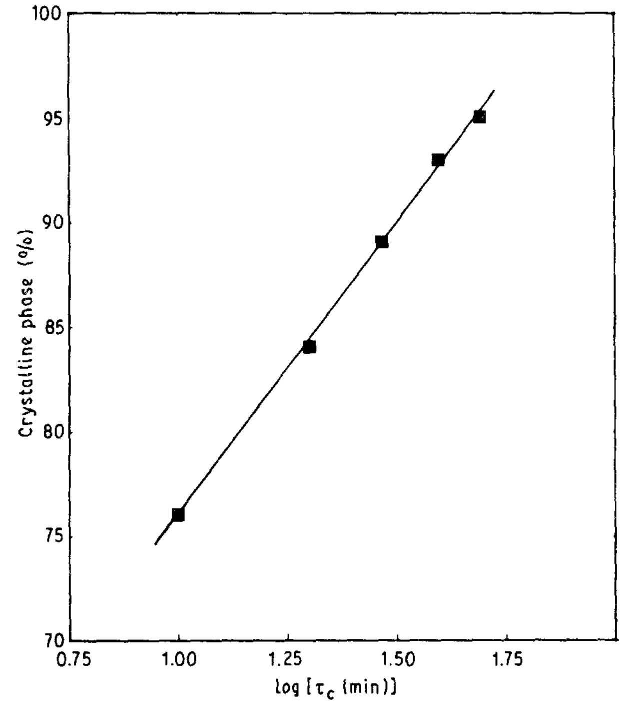

Figure 7 Crystalline phase percentage versus log τ_c.

The crystalline phase percentage (%CPh) as a function of the holding time (τ_c) at the crystallization temperature (T_c) (830 ± 10 °C) was determined by the image analysis technique for the B composition of GC. The small grain size shown by compositions C and D did not allow reliable discrimination between the voids, left by dissolution of the G, and the crystals. The crystalline phase percentage and the thermal treatment duration are listed in Table III.

By least-squares treatment of the experimental data the following regression is obtained:

$$\%\text{CPh} = (27.94 \pm 0.16)\log \tau_c + (48.84 \pm 0.32)$$

where the associated error is the standard deviation from the mean. The same data are depicted in Fig. 7. The validity of the relation between thermal treatment duration and percentage of crystallinity can be considered reliable from 10 to 60 min.

4. Conclusions

On the basis of the experimental data obtained in this study the following conclusions can be suggested:

1. The chemical compositions of the batches (A, B, C, D) investigated are suitable for glass-forming under air-cooling conditions. The T–T–T curve shows that the minimum stability of the G phase corresponds to ~ 640 °C.
2. The minimum amount of nucleating agents (TiO_2 + ZrO_2) needed for an efficient bulk nucleation, and subsequent growth of fine crystals, is not less than 4.5%. With this percentage and the appropriate thermal treatment, the grain size is less than 0.1 µm.
3. By increasing the percentage of nucleating agents the crystallization temperature is lowered and the size of the crystalline grains is modified (due to the more efficient nucleation process), while the nature of the precipitated phase remains the same.
4. The coupled SEM and image analysis techniques are effective and reliable for measuring the ratio between the amorphous and crystalline phases if the grain size is in the region of 1 µm. For smaller crystals alternative techniques, such as the X-ray diffraction analysis of standard samples, must be used.

It must be pointed out that this technique cannot be used universally, because solvents that will sufficiently differentiate the phases cannot always be found. For our Li_2O–Al_2O_3–SiO_2 type of GC, the G phase is soluble in HF while the crystal phase is not.

Acknowledgements

The authors are sincerely grateful to the Consiglio Nazionale delle Ricerche for financial support and to Ms Ida Ferrante and Emanuela Antenucci for collaboration in the experimental work.

References

1. P. W. McMILLAN, in "Glass Ceramics" (Academic, London, 1979) p. 223.
2. Z. STRNAD, in "Glass Science and Technology" (Elsevier, Amsterdam, 1986) p. 85.
3. G. PARTRIDGE, *Glass Technol.* **23** (1982) 3.
4. G. H. BEALL, in "Advances in Ceramics", Vol. 18 (American Ceramic Society, Columbus, Ohio, 1986) p. 157.
5. D. R. STEWART, in "Advances in Nucleation and Crystallization of Glasses" (American Ceramic Society, Columbus, Ohio, 1971) p. 5.
6. A. MAROTTA, A. BURI and F. BRANDA, *Thermochim. Acta* **40** (1980) 397.
7. A. MAROTTA, S. SCIELLO, F. BRANDA and A. BON, *J. Mater. Sci.* **17** (1982) 105.
8. V. MAIER and G. MULLER, *J. Amer. Ceram. Soc.* **70** (1987) C-176.

Received 13 August
and accepted 20 December 1990